SIAM J. NUMER. ANAL.
Vol. 23, No. 3, June 1986

SPLIT-STEP METHODS FOR THE SOLUTION OF THE NONLINEAR SCHRÖDINGER EQUATION*

J. A. C. WEIDEMAN† AND B. M. HERBST†

Abstract. A split-step method is used to discretize the time variable for the numerical solution of the nonlinear Schrödinger equation. The space variable is discretized by means of a finite difference and a Fourier method. These methods are analyzed with respect to various physical properties represented in the NLS. In particular it is shown how a conservation law, dispersion and instability are reflected in the numerical schemes. Analytical and numerical instabilities of wave train solutions are identified and conditions which avoid the latter are derived. These results are demonstrated by numerical examples.

Key words. split-step, nonlinear Schrödinger equation, modulational instability, recurrence, conservation laws

AMS(MOS) subject classifications. Primary 65M10, secondary 65M99

1. Introduction. Only fairly recently it was realized that weakly nonlinear periodic wave trains on deep water are unstable. The earlier results on this phenomenon (for example, see [1]) were only valid for the initial growth period of the instabilities. Subsequent investigations indicated that the time evolution of the modulation of these wave trains is described by the nonlinear Schrödinger equation (NLS) [2], [3], [4]

$$iu_t + u_{xx} + q|u|^2 u = 0, \qquad -\infty < x < \infty. \tag{1a}$$

Here u is a complex valued function, q a real parameter and $i^2 = -1$.

Theoretical, experimental and numerical investigations have since confirmed the validity of the NLS for a description of modulations of deep water waves [5], [6], [7]. For example, Lake et al. [6] and Yuen et al. [7] solved the NLS numerically and verified the instability of the solution. In addition, they found that the instability does not grow unboundedly as expected in linear theory, but that the conservation laws satisfied by the NLS tend to inhibit the growth. The result is that the solution returns to the initial condition periodically. This phenomenon was also observed in wave tank experiments and is known as recurrence. Originally, this remarkable feature of some nonlinear problems was encountered in another context by Fermi, Pasta and Ulam [8]. A particularly useful overview of these developments is given by Yuen and Lake [9]. In addition, the NLS has also found application in other fields such as nonlinear optics and plasma physics [3], [4].

Apart from its physical significance the NLS is of considerable interest to the numerical analyst in its own right. Some of its features which attract the numerical analyst are: nonlinearity and dispersion which under favourable conditions allow soliton solutions [10], instability and recurrence [7], as well as bound states of two or more solitons [11] whose steep spatial and temporal gradients pose a real challenge to numerical methods [12].

Among the earlier methods used for solving the NLS numerically, are split-step and Fourier methods, for example the methods employed by Lake et al. [6] and Tappert [13]. Some of the more recent references to numerical solutions of the NLS include [14]–[20]. These authors used mainly finite difference or finite element methods to

* Received by the editors November 12, 1984, and in revised form April 30, 1985.

† Department of Applied Mathematics, University of the Orange Free State, Bloemfontein 9300, South Africa.

discretize the space variable. For the discretization of the time variable, Sanz-Serna [14], [15] used an explicit, variable time step, leapfrog scheme, Delfour et al. [16] a modified Crank–Nicolson scheme, Griffiths et al. [17] a predictor-corrector method and Herbst et al. [18] the midpoint rule.

Recently Taha and Ablowitz [21] conducted extensive computations in which the split-step Fourier method of Tappert [13] was compared with several finite difference, pseudospectral and even global methods, including some of the methods described in [14]–[20]. In the majority of their experiments the split-step method turned out to be superior. The method owes part of its success to the fact that it avoids solving a nonlinear algebraic system at each time level. Thus high accuracy may be obtained at comparatively low computational cost. Despite this advantage over many of its rivals, fairly little is known about the theoretical behaviour of the split-step method as applied to the NLS. The aim of this report is therefore to analyze some aspects of the split-step method for the numerical solution of the NLS. For analyses with application to related problems, the reader is referred to [22]–[24] for split-step and to [25]–[27] for Fourier methods.

In the numerical study of the NLS there are two types of solutions which attract much interest. The first type is the soliton solutions, in which the solution and its spatial derivatives vanish at $x = \pm\infty$. The second type is the solutions which describe modulational instability and recurrence and where periodic boundary conditions are appropriate. In this report we shall only discuss the latter type of problem and thus restrict ourselves to L-periodic solutions defined by

$$u(x+L, t) = u(x, t), \qquad -\infty < x < \infty, \quad t > 0. \tag{1b}$$

In § 3 time integration by the split-step method will be discussed. It will be shown that in the case of the NLS, this procedure has the effect that the problem becomes explicit in the nonlinear part. Hence the inexpensive computation mentioned earlier. For simplicity we only discuss two ways of discretizing the space variable, namely a finite difference (§ 4) and a Fourier method (§ 5). The latter method is due to Tappert [13].

With our theoretical investigations we adopted the approach that the salient physical properties of the NLS should also be reflected in the numerical schemes. In this report our investigations are concerned with the conservation of energy, the nonlinear dispersion relation and the (linearized) stability of the numerical methods. In particular we show that the schemes are energy conserving. Also the discrete form of the nonlinear dispersion relation will be shown to be exact in the case of the Fourier method, and a good approximation to the analytical relation in the case of the finite difference method, provided a suitably fine grid is used. As far as stability is concerned, we shall indicate that the methods are able to simulate closely the analytical instability properties of the NLS. However, it is also found that the numerical schemes are more unstable than the analytical problem, in the sense that instabilities are obtained which have no analytical counterpart. Care should therefore be exercised if a problem such as recurrence is to be investigated, since some instabilities may be of numerical origin. Stepsize restrictions to avoid the numerical instabilities will be derived in §§ 4 and 5. These restrictions will be verified numerically in § 6.

One point we would like to stress is that our instability analyses are solely concerned with the unsteady solutions of the NLS associated with disturbances on a uniform wave train. Solutions of this form readily lead to linearization by which means the instability will be investigated. Therefore the essential nonlinear behaviour of the problem cannot be explained in full. For example, the appearance of instabilities on

a uniform wave train is predicted by the linearization methods we employ, provided the perturbations are small. On the other hand, the long time behaviour and the return to the initial state when recurrence occurs fall outside the scope of these analyses. However, we shall show by numerical experiment that linearization proves to be remarkably accurate in predicting instabilities introduced by rounding error.

We start by stating some of the relevant analytical properties of the NLS.

2. Analytical properties of the NLS. It will be convenient to rewrite (1a) as

$$u_t = i\mathcal{L}u + i\mathcal{N}(u)u, \qquad -\infty < x < \infty, \tag{2a}$$

where

$$\mathcal{L}u := u_{xx}, \qquad \mathcal{N}(u) := q|u|^2. \tag{2b}$$

2.1. Conservation. Only one of the infinite number of conservation laws satisfied by the solution of the NLS will be of concern to us. This is the conservation of energy given by

$$\frac{d}{dt}\int |u|^2\,dx = 0 \tag{3}$$

where the integration is performed over a one-period interval.

2.2. Dispersion. Consider a periodic wave train with constant amplitude a, wave number k, and frequency ω, namely

$$u(x, t) = a \exp i(kx - \omega t). \tag{4}$$

This is a solution of (2), provided the following dispersion relation is satisfied

$$\omega = k^2 - q|a|^2. \tag{5}$$

The fact that the amplitude is involved in the dispersion relation, is typical of nonlinear waves [4]. This causes the solution to become unstable under certain conditions, as we now proceed to show.

2.3. Instability. Consider a solution of the NLS of the form

$$\mathring{u}(x, t) := a \exp i(kx - \omega t) \tag{6}$$

with ω given by (5). In order to investigate the stability of this uniform wave train, we consider a perturbed solution of the form

$$u(x, t) = \mathring{u}(x, t)(1 + \varepsilon(x, t)) \tag{7}$$

where $|\varepsilon|^2 \ll 1$. Substitution of (7) into (2a) and retaining first order terms in ε, yield

$$\varepsilon_t = i\varepsilon_{xx} - 2k\varepsilon_x + iq|a|^2(\varepsilon + \varepsilon^*) \tag{8}$$

where * denotes the complex conjugate.

We assume that ε is periodic on the interval $[-\frac{1}{2}L, \frac{1}{2}L]$, and express it as the Fourier series

$$\varepsilon(x, t) = \sum_{n=-\infty}^{\infty} \hat{\varepsilon}_n(t) \exp(i\mu_n x) \tag{9}$$

where

$$\mu_n = 2\pi n / L. \tag{10}$$

From (8) and (9) the following systems of ordinary differential equations are obtained

$$\frac{d}{dt}\begin{pmatrix}\hat{\varepsilon}_n\\ \hat{\varepsilon}^*_{-n}\end{pmatrix} = G_n\begin{pmatrix}\hat{\varepsilon}_n\\ \hat{\varepsilon}^*_{-n}\end{pmatrix}, \qquad n=-\infty,\cdots,\infty,\ n\neq 0, \tag{11}$$

where

$$G_n := i\begin{pmatrix} q|a|^2-2k\mu_n-\mu_n^2 & q|a|^2\\ -q|a|^2 & -q|a|^2-2k\mu_n+\mu_n^2\end{pmatrix}.$$

The eigenvalues λ_n of G_n are given by

$$\lambda_n = -2ik\mu_n \pm \mu_n\sqrt{2q|a|^2-\mu_n^2}.$$

One of the eigenvalues has a positive real part and accordingly $(\hat{\varepsilon}_n, \hat{\varepsilon}^*_{-n})^T$ will grow exponentially if

$$0<\mu_n^2<2q|a|^2. \tag{12}$$

Thus we have shown that if the perturbed solution (7) contains both side-band modes $k+\mu_n$ and $k-\mu_n$ which are close enough to the fundamental mode k so that (12) is satisfied, then the perturbation will grow exponentially in the initial stages.

It is clear that the instability is caused by the nonlinear term in the NLS, and it can only occur if $q>0$.

We now turn to the numerical solution of the NLS, and we start by discussing the discretization of the time variable.

3. The split-step method. The solution of (2) may be advanced from one time-level to the next by means of the following formula

$$u(x,\, t+\tau)\approx \exp i\tau(\mathscr{L}+\mathscr{N}(u))\cdot u(x,\, t), \tag{13}$$

where τ denotes the time step. In general (13) is first order accurate, but under special circumstances $|u|^2$ is time-independent in which case (13) turns out to be exact.

The time-splitting procedure now consists of replacing the right-hand side of (13) by

$$\exp\,(i\tau(\mathscr{L}+\mathscr{N}(u))\cdot u(x,\, t)\approx \exp i\tau\mathscr{L}\cdot\exp i\tau\mathscr{N}(u)\cdot u(x,\, t). \tag{14}$$

This expression is exact whenever $\mathscr{L}$ and $\mathscr{N}$ commute. Otherwise the splitting is first order accurate. Accordingly, we use

$$U(x,\, t+\tau)=\exp i\tau\mathscr{L}\cdot\exp i\tau\mathscr{N}(U)\cdot U(x,\, t) \tag{15}$$

where $U(x,\, t)$ denotes the approximation of $u(x,\, t)$.

Incidentally, some authors find it convenient to view the scheme (15) as successively solving the equations

$$u_t = i\mathscr{N}(u)u, \qquad u_t = i\mathscr{L}u$$

employing the solution of the former equation as initial condition for the latter.

Next, we introduce the quantity

$$V^m := \exp i\tau\mathscr{N}(U^m)\cdot U^m \tag{16}$$

where U^m denotes the approximation at the time $m\tau$. Then the split-step scheme (15) may be written as

$$U^{m+1}=\exp i\tau\mathscr{L}\cdot V^m. \tag{17}$$

We shall refer to the quantity V^m as an intermediate solution, although it cannot be considered an approximation to the theoretical solution. We observe, however, that if U^m is L-periodic, so is V^m, and therefore the boundary conditions are not violated by the introduction of an intermediate step.

For possible extension of the split-step method to second order accuracy the reader is referred to Strang [22] and Sanz-Serna and Verwer [29].

Since the operator $\mathcal{N}$ of the NLS does not involve derivatives, no further approximation to (16) need be made. On the other hand, the formula (17) involves the second space derivative and approximation in space is required for computation. We now turn to this discretization of the space variable, and in the following section we consider a finite difference method for this purpose.

4. Finite difference methods. Although the NLS equation is defined over the real line we need to impose conditions at a finite boundary when it is solved numerically. Since in this report we are only concerned with L-periodic solutions of the NLS we impose periodic conditions at $[-\frac{1}{2}L, \frac{1}{2}L]$. This interval is divided in N equal subintervals with grid spacing h, i.e.

$$h := \frac{L}{N}. \tag{18a}$$

The grid points are denoted by

$$x_j = jh, \qquad j = -\frac{N}{2}, \cdots, \frac{N}{2}. \tag{18b}$$

The approximation of $u(x_j, m\tau)$ is denoted by U_j^m.

In order to implement the split-step scheme (16)-(17) in practice, we use the following well-known rational approximation

$$\exp i\tau\mathcal{L} = (\mathcal{I} - \theta i\tau\mathcal{L})^{-1}(\mathcal{I} + (1-\theta)i\tau\mathcal{L}) \tag{19}$$

where $\mathcal{I}$ is the identity operator and θ is a free parameter with $0 \leqq \theta \leqq 1$.

Equation (17) now becomes

$$(\mathcal{I} - \theta i\tau\mathcal{L})U^{m+1} = (\mathcal{I} + (1-\theta)i\tau\mathcal{L})V^m. \tag{20}$$

The space variable may be discretized by replacing $\mathcal{L}$ by $\mathcal{L}_h$, where

$$\mathcal{L}_h U_j := (U_{j+1} - 2U_j + U_{j-1})/h^2, \qquad j = -N/2, \cdots, N/2-1 \tag{21}$$

and where

$$U_{-N/2-1} := U_{N/2-1}, \qquad U_{N/2} := U_{-N/2}$$

to ensure a periodic solution. Hence the scheme (20) may be written in matrix notation as

$$(I - ir\theta S)\mathbf{U}^{m+1} = (I + ir(1-\theta)S)\mathbf{V}^m \tag{22}$$

where I is the identity matrix, and

$$r := \frac{\tau}{h^2}, \qquad \mathbf{U} := (U_{-N/2}, \cdots, U_{N/2-1})^T, \tag{23}$$

$$V_j^m := \exp(i\tau q|U_j^m|^2) \cdot U_j^m, \tag{24}$$

and

$$S := \begin{pmatrix} -2 & 1 & & \cdot & \cdot & 1 \\ 1 & -2 & 1 & & & \cdot \\ \cdot & 1 & -2 & 1 & & \cdot \\ \cdot & \cdot & \cdot & \cdot & \cdot & \cdot \\ \cdot & & 1 & -2 & 1 & \cdot \\ \cdot & & & 1 & -2 & 1 \\ 1 & \cdot & \cdot & \cdot & 1 & -2 \end{pmatrix}$$

where only the nonzero entries have been shown.

We shall refer to the scheme (22) as the split-step finite difference scheme. Because of the $O(\tau)$ accuracy of the splitting stage of the procedure and the $O(h^2)$ accuracy when $\mathscr{L}$ is replaced by $\mathscr{L}_h$, the accuracy of the scheme is $O(\tau+h^2)$. Although the scheme (22) is implicit, we need not solve a nonlinear algebraic system of equations at each time level. Since the matrix on the left-hand side of (22) is time-independent and quasi-tridiagonal the system can be solved very efficiently by an optimization of Gaussian elimination (for details, see Taha and Ablowitz [21]).

4.1. Conservation. In this section we show that the free parameter θ in the scheme (22) may be fixed by the requirement that a discrete analogue of the conservation of energy (3) has to be satisfied.

We rewrite (22) as

$$\mathbf{U}^{m+1}-\mathbf{V}^m = ir[\theta S\mathbf{U}^{m+1}+(1-\theta)S\mathbf{V}^m]$$

and pre-multiply it with

$$(\mathbf{U}^{m+1}*+\mathbf{V}^m*)^T.$$

If the real part of the result is taken, we obtain with the aid of (24)

$$(25)\quad (\mathbf{U}^{m+1}*)^T\mathbf{U}^{m+1}-(\mathbf{U}^m*)^T\mathbf{U}^m = \mathrm{Re}\,\{[\mathbf{U}^{m+1}*+\mathbf{V}^m*]^T irS[\theta\mathbf{U}^{m+1}+(1-\theta)\mathbf{V}^m]\}.$$

It is easily verified that

$$\mathrm{Im}\,(\mathbf{W}^{*T}S\mathbf{W}) = 0$$

for any complex vector $\mathbf{W}$. It therefore follows that the right-hand side of (25) vanishes provided

$$(26)\qquad \theta = \tfrac{1}{2}.$$

The discrete form of the conservation law (3) satisfied by the split-step finite difference scheme is therefore given by

$$(27)\qquad h\sum_j |U_j^m|^2 = h\sum_j |U_j^{m+1}|^2, \qquad m = 0, 1, 2, \cdots.$$

Because of this desirable property, the choice (26) will henceforth be used.

4.2. Dispersion. A discrete analogue of the nonlinear dispersion relation (5) may be obtained if we assume a solution of (22) (with $\theta = \frac{1}{2}$) of the form

$$(28)\qquad U_j^m = a\exp i(kx_j - \omega m\tau).$$

Substitution of (28) into (22) yields

$$(29)\qquad \exp i\omega\tau = (1+irs)^{-1}(1-irs)\exp(-iq|a|^2\tau)$$

where

$$s := \cos kh - 1.$$

From (29) it follows that

(30a) $$\omega = -\left(\frac{2\phi}{\tau}\right) - q|a|^2$$

where

(30b) $$\cos\phi := \frac{1}{\sqrt{1+r^2s^2}}, \qquad \sin\phi := \frac{rs}{\sqrt{1+r^2s^2}}.$$

In order to compare (30a) and (5) we fix r and consider the limits

$$kh \to 0, \qquad \tau \to 0.$$

A Taylor expansion yields

$$\phi = -\tfrac{1}{2}rk^2h^2 + O(k^4h^4)$$

where the constant implied by the $O(k^4h^4)$ term depends on r but not on h or τ separately. Thus we obtain

(31) $$\omega = k^2 - q|a|^2 + O(k^4h^2).$$

We see that the discrete relation (30a) tends to the exact relation as $h, \tau \to 0$. Also note that (31) is only a good approximation of (5) if k^4h^2 is small. This confirms the intuitive notion that a highly oscillatory problem should be solved on a fine grid. In the case $k = 0$, (5) and (30a) are identical. Thus, if computational errors are not taken into account, the split-step finite difference scheme is able to solve the x-independent solution of the NLS exactly.

4.3. Instability. In this section we investigate the manner in which the analytical instability, outlined in § 2.3, is reflected in the split-step finite difference scheme. For simplicity we restrict ourselves to the x-independent solution,

(32) $$\mathring{U}^m := a \exp(iq|a|^2 m\tau)$$

which corresponds to $k = 0$ in (6). Following the analytical procedure (32) is now perturbed to

(33) $$U_j^m = \mathring{U}^m(1 + \varepsilon_j^m)$$

where

$$|\varepsilon_j^m|^2 \ll 1.$$

We substitute (33) into (24) and ignore second order terms in ε_j^m to obtain

(34) $$V_j^m = \mathring{U}^{m+1}[1 + \varepsilon_j^m + iq|a|^2\tau(\varepsilon_j^m + \varepsilon_j^{m*})].$$

Upon substitution of (34) and (33) at $t = (m+1)\tau$ into the split-step scheme (22) we have

(35) $$\left(1 - \frac{i\tau}{2}\mathscr{L}_h\right)\varepsilon_j^{m+1} = \left(1 + \frac{i\tau}{2}\mathscr{L}_h\right)[(1 + iq|a|^2\tau)\varepsilon_j^m + iq|a|^2\tau\varepsilon_j^{m*}]$$

where $\mathscr{L}_h$ is defined by (21).

If we now assume the perturbation ε_j^m to be periodic on the interval $[-\frac{1}{2}L, \frac{1}{2}L]$ we may express it as the discrete Fourier series

$$\varepsilon_j^m = \sum_{n=-N/2}^{N/2-1} \hat{\varepsilon}_n^m \exp(i\mu_n x_j) \tag{36a}$$

with frequencies

$$\mu_n := \frac{2\pi n}{L}. \tag{36b}$$

By substituting (36a) into (35) and collecting terms in $\exp(i\mu_n x_j)$ and $\exp(-i\mu_n x_j)$ we obtain

$$\begin{pmatrix} \hat{\varepsilon}_n \\ \hat{\varepsilon}_{-n}^* \end{pmatrix}^{m+1} = A_n \begin{pmatrix} \hat{\varepsilon}_n \\ \hat{\varepsilon}_{-n}^* \end{pmatrix}^m, \qquad n = -N/2, \cdots, N/2-1, \quad n \neq 0$$

where the amplification matrices are given by

$$A_n := \begin{pmatrix} d_n(1+iq|a|^2\tau) & d_n iq|a|^2\tau \\ -d_n^{-1} iq|a|^2\tau & d_n^{-1}(1-iq|a|^2\tau) \end{pmatrix}$$

where

$$d_n := \frac{1+irs_n}{1-irs_n}, \quad r := \tau/h^2, \quad s_n := \cos\mu_n h - 1.$$

The eigenvalues of A_n are given by

$$\lambda_n = \beta_n \pm (\beta_n^2 - 1)^{1/2} \tag{37}$$

where

$$\beta_n := \frac{(1 - r^2 s_n^2 - 2q|a|^2 \tau r s_n)}{(1 + r^2 s_n^2)}$$

Exponential growth will be exhibited by $(\hat{\varepsilon}_n, \hat{\varepsilon}_{-n}^*)^T$ whenever either of the eigenvalues given by (37), satisfies

$$|\lambda_n| > 1.$$

This is equivalent to

$$|\beta_n| > 1$$

and we obtain two conditions for instability, namely

$$0 < \frac{2}{h^2} \sin^2\left(\frac{\mu_n h}{2}\right) < q|a|^2 \tag{38}$$

and

$$2q|a|^2\tau^2 h^{-2} \sin^2\left(\frac{\mu_n h}{2}\right) < -1. \tag{39}$$

The first condition can only be satisfied if $q > 0$. It therefore corresponds to the analytical result (12). Indeed, we have from (38) that

$$0 < \mu_n^2 < 2q|a|^2 + O(h^2).$$

The exact number of unstable modes in the Fourier series (36a) is given by the largest

integer n which satisfies

$$\frac{2N^2}{L^2}\sin^2\frac{\pi n}{N} < q|a|^2. \tag{40}$$

We further note that if

$$h > \left(\frac{2}{q|a|^2}\right)^{1/2} \tag{41}$$

all modes are unstable according to (38). For instance, consider a random rounding error which may be expected to contain all frequencies. Because of the large value of h all modes of this perturbation will be magnified in the same way as the analytically unstable modes. Severe instability of a uniform wave train solution may thus be expected if (41) is satisfied.

The second instability condition (39) can only be satisfied if $q<0$. It therefore has no analytical counterpart and is a purely numerical phenomenon. It may be prevented by using

$$\tau < (2|q|\,|a|^2)^{-1/2}h. \tag{42}$$

We also note that the condition

$$|\beta_n| \leqq 1$$

implies

$$|\lambda_n| = 1$$

for both eigenvalues given by (37). Accordingly the method is neutrally stable when neither (38) nor (39) is satisfied.

A final observation is that when (39) is satisfied, the high frequency Fourier components in (36a) are likely to be unstable. When (38) is satisfied, it is the low frequency components which are unstable. Because the high frequency instability has no analytical counterpart we shall refer to it as numerical instability.

5. A Fourier method. In this section, the space discretization is accomplished by a Fourier method. We first recall a few well-known results concerning discrete Fourier transforms (see e.g. Conte and de Boor [30]).

Let $w(x)$ be a L-periodic function, i.e. $w(x+L)=w(x)$. The Fourier-series of $w(x)$ is given by

$$w(x) = \sum_{n=-\infty}^{\infty} \hat{w}_n \exp(i\mu_n x) \tag{43}$$

where μ_n is given by (36b) and the Fourier coefficients $\hat{w}_n$ by

$$\hat{w}_n = \frac{1}{L}\int_{-L/2}^{L/2} w(x)\exp(-i\mu_n x)\,dx. \tag{44}$$

The interval $[-L/2, L/2]$ is divided into N equal subintervals as before with grid spacing h and grid points x_j given by (18a) and (18b), respectively. The discrete Fourier transform of the discrete function

$$\mathbf{W} := (W_{-N/2}, \cdots, W_{N/2-1})^T$$

is defined by

$$\hat{W}_n := \frac{h}{L}\sum_j W_j \exp(-i\mu_n x_j), \qquad n = -N/2, \cdots, N/2-1. \tag{45}$$

Here, and in the remainder of this section summation indices range from $-N/2$ to $N/2-1$ unless otherwise stated. The inverse formula is

$$W_j := \sum_n \hat{W}_n \exp(i\mu_n x_j), \qquad j = -N/2, \cdots, N/2-1. \tag{46}$$

If $\mathbf{W}$ is obtained from $w(x)$ by means of

$$W_j = w(x_j)$$

then the following relationship exists between $\hat{W}_n$ and $\hat{w}_n$ as defined by (45) and (44)

$$\hat{W}_n = \sum_{j=-\infty}^{\infty} \hat{w}_{n+jN}, \qquad n = -N/2, \cdots, N/2-1. \tag{47}$$

In addition if $w(x)$ has $k-1$ continuous derivatives and piecewise continuous kth derivative then

$$\hat{W}_j = \hat{w}_j + O(h^k). \tag{48}$$

The first step in the Fourier split-step scheme now consists of replacing $V^m(x)$ and $U^{m+1}(x)$ in (17) by their Fourier series. This yields

$$\hat{u}_n^{m+1} = \exp(-i\mu_n^2 \tau)\hat{v}_n^m, \qquad n = -\infty, \cdots, \infty \tag{49}$$

where the $\hat{v}_n^m$ and $\hat{u}_n^{m+1}$ are the Fourier coefficients of the continuous functions $V^m(x)$ and $U^{m+1}(x)$, respectively. Equation (49) may now be "discretized" by replacing $\hat{v}_n^m$ by $\hat{V}_n^m$ where

$$\hat{V}_n^m = \frac{h}{L} \sum_j V_j^m \exp(-i\mu_n x_j), \qquad n = -N/2, \cdots, N/2-1 \tag{50}$$

and where V_j^m is the intermediate solution given by (24). Thus, (49) becomes

$$\hat{U}_n^{m+1} = \exp(-i\mu_n^2 \tau)\hat{V}_n^m, \qquad n = -N/2, \cdots, N/2-1. \tag{51}$$

Finally the approximation at the next time level is calculated from the inverse transform

$$U_j^{m+1} = \sum_n \hat{U}_n^{m+1} \exp(i\mu_n x_j), \qquad j = -N/2, \cdots, N/2-1. \tag{52}$$

Equation (47) shows that if our solution is band-limited, i.e. if there exists an n_0 such that

$$\hat{u}_n^m = 0, \qquad |n| > n_0$$

then the Fourier discretization is exact provided

$$N \geqq 2n_0. \tag{53}$$

However we still only have first order accuracy in time. In order to render the method competitive as far as speed of computation is concerned, the transforms (50) and (52) should be computed by Fast Fourier techniques [31].

We note that the Fourier method is only applicable to periodic problems, whereas the finite difference method of the previous section may easily be modified to cope with more general problems. In practice, however, this does not turn out to be a major drawback of the Fourier method. For example, if a problem with soliton solutions has to be solved, the boundaries are merely placed far enough apart in order not to interfere with the wave motion.

We now investigate the conservation, dispersion and instability properties of the split-step Fourier method.

5.1. Conservation. To prove conservation of energy for the split-step Fourier scheme (50), (51), we require the discrete form of Parseval's relation, given by

$$\frac{h}{L}\sum_j |W_j|^2 = \sum_j |\hat{W}_j|^2 \tag{54}$$

where W_j and $\hat{W}_j$ are related through (45).

From (24) and (54) it follows that

$$\sum_j |U_j^m|^2 = \sum_j |V_j^m|^2 = \frac{L}{h}\sum_j |\hat{V}_j^m|^2.$$

From (51) and a second application of Parseval's relation we obtain

$$\frac{L}{h}\sum_j |\hat{V}_j^m|^2 = \frac{L}{h}\sum_j |\hat{U}_j^{m+1}|^2 = \sum_j |U_j^{m+1}|^2.$$

Hence

$$h\sum_j |U_j^m|^2 = h\sum_j |U_j^{m+1}|^2, \qquad m = 0, 1, 2, \cdots \tag{55}$$

which is a discrete analogue of (3).

5.2. Dispersion. Again we assume a solution of the form

$$U_j^m = a \exp i(kx_j - \omega m\tau). \tag{56}$$

This implies a periodicity L of U_j^m where $L = 2\pi/k$, and from (36b) we get $\mu_n = nk$. Direct evaluation of (50) and (51) now yields

$$\hat{V}_n^m = \begin{cases} 0, & n \neq 1, \\ a \exp i(-\omega m\tau + q|a|^2\tau), & n = 1 \end{cases} \tag{57a}$$

and

$$\hat{U}_n^{m+1} = \begin{cases} 0, & n \neq 1, \\ a \exp i(-\omega m\tau + q|a|^2\tau - k^2\tau), & n = 1. \end{cases} \tag{57b}$$

The inverse transform of (57b) gives

$$U_j^{m+1} = a \exp i(kx_j - \omega m\tau + q|a|^2\tau - k^2\tau)$$

and this is equal to

$$U_j^{m+1} = a \exp i(kx_j - \omega(m+1)\tau)$$

provided

$$\omega = k^2 - q|a|^2.$$

This is identical to the analytical dispersion relation (5). The fact that an exact expression is obtained is a direct consequence of (53) which, in this case, shows that no error in the space discretization is committed, provided

$$N \geq 2.$$

Furthermore, since $|U|^2$ is independent of x and t the expression (13) is exact; $\mathscr{L}$ and $\mathscr{N}$ commute which imply that the time discretization (15) is also exact. Hence the Fourier split-step scheme solves the uniform wave train solution (4) exactly, provided

no computational errors are introduced. Of course, in practice computational errors are expected. Therefore we turn to a stability analysis to establish under which conditions perturbations, for example numerical errors, may grow.

5.3. Instability. We consider the stability of the x-independent or $k=0$ solution,

$$\mathring{U}^m := a \exp(iq|a|^2 m\tau) \tag{58}$$

of the Fourier split-step method. We perturb (58) to

$$U_j^m = \mathring{U}^m(1+\varepsilon_j^m) \tag{59}$$

where ε_j^m is assumed to be a L-periodic function. The discrete Fourier expansion of the perturbation is

$$\varepsilon_j^m := \sum_n \hat{\varepsilon}_n^m \exp(i\mu_n x_j), \qquad j=-N/2,\cdots,N/2-1, \tag{60}$$

where μ_n is given by (36b).

As in § 4.3, we substitute (59) into (24) and retain first order terms in ε_j^m, to arrive at the linearized version of the intermediate solution (34).

From (34) and (50) it follows that

$$\hat{V}_n^m = \begin{cases} \mathring{U}^{m+1}[1+(1+iq|a|^2\tau)\hat{\varepsilon}_0^m + iq|a|^2\tau\hat{\varepsilon}_0^{m*}], & n=0, \\ \mathring{U}^{m+1}[(1+iq|a|^2\tau)\hat{\varepsilon}_n^m + iq|a|^2\tau\hat{\varepsilon}_{-n}^{m*}], & n\neq 0. \end{cases} \tag{61}$$

Next $\hat{U}_n^{m+1}$ is computed from (51) and (61), to give

$$\hat{U}_n^{m+1} = \begin{cases} \mathring{U}^{m+1}[1+(1+iq|a|^2\tau)\hat{\varepsilon}_0^m + iq|a|^2\tau\hat{\varepsilon}_0^{m*}], & n=0, \\ \mathring{U}^{m+1}[(1+iq|a|^2\tau)\exp(-i\mu_n^2\tau)\hat{\varepsilon}_n^m + iq|a|^2\tau\exp(-i\mu_n^2\tau)\hat{\varepsilon}_{-n}^{m*}], & n\neq 0. \end{cases} \tag{62}$$

On the other hand, from (59) and (60) we have

$$\hat{U}_n^{m+1} = \begin{cases} \mathring{U}^{m+1}(1+\hat{\varepsilon}_0^{m+1}), & n=0, \\ \mathring{U}^{m+1}\hat{\varepsilon}_n^{m+1}, & n\neq 0. \end{cases} \tag{63}$$

A comparison of (62) and (63) yields

$$\begin{pmatrix} \hat{\varepsilon}_n \\ \hat{\varepsilon}_{-n}^* \end{pmatrix}^{m+1} = A_n \begin{pmatrix} \hat{\varepsilon}_n \\ \hat{\varepsilon}_{-n}^* \end{pmatrix}^m, \qquad n=-\frac{N}{2},\cdots,\frac{N}{2}, \quad n\neq 0$$

where the amplification matrices A_n are given by

$$A_n := \begin{pmatrix} (1+iq|a|^2\tau)\exp(-i\mu_n^2\tau) & iq|a|^2\tau\exp(-i\mu_n^2\tau) \\ -iq|a|^2\tau\exp(i\mu_n^2\tau) & (1-iq|a|^2\tau)\exp(i\mu_n^2\tau) \end{pmatrix}.$$

As in § 4.3, the eigenvalues of A_n are given by an expression of the form (37), with β_n given by

$$\beta_n := \cos\mu_n^2\tau + q|a|^2\tau\sin\mu_n^2\tau. \tag{64}$$

Thus the condition for instability becomes

$$|\cos\mu_n^2\tau + q|a|^2\tau\sin\mu_n^2\tau| > 1. \tag{65}$$

This is equivalent to

$$|\cos(\mu_n^2\tau-\theta)| > \cos\theta \tag{66a}$$

where

$$\cos\theta := \frac{1}{\sqrt{1+q^2|a|^4\tau^2}}, \qquad \sin\theta := \frac{q|a|^2\tau}{\sqrt{1+q^2|a|^4\tau^2}}. \tag{66b}$$

One of the inequalities implied by (65) is $\beta_n > 1$, and a Taylor-expansion shows that

$$0 < \mu_n^2 < 2q|a|^2 + O(\tau). \tag{67}$$

This result is clearly consistent with the analytical result (12).

The fact that (67) does not involve the space discretization is easily explained. From (60) we see that the perturbed solution is band-limited with $n_0 = N/2$. Comparison with (53) shows that no error is made in the spatial approximation.

Because of the oscillatory nature of the instability condition (66a), some high frequency modes may be unstable, in addition to the low frequency modes given by (67). To see this, we consider $q|a|^2$ and τ fixed, i.e., θ fixed, and define

$$g(\mu^2) = \cos(\mu^2\tau - \theta).$$

It will be convenient to consider μ as a continuous variable, even though the frequencies present in the computation can only assume the discrete values $\mu_n = 2\pi n/L$. We note that if $q > 0$ then $0 < \theta < \pi/2$, and if $q < 0$ then $-\pi/2 < \theta < 0$.

The function g has turning points at

$$\mu^2 = \mu_p^2 := \frac{\theta + p\pi}{\tau}, \qquad p = 0, 1, \cdots \tag{68}$$

with $p = 0$ excluded in the case $q < 0$.

It follows that the inequalities

$$|g(\mu^2)| > \cos\theta \tag{69a}$$

and

$$|\mu^2 - \mu_p^2| < \frac{|\theta|}{\tau}, \qquad p = 0, 1, \cdots \tag{69b}$$

are equivalent. Thus, whenever $\mu = \mu_n$ satisfies (69b) for some p, the nth mode becomes unstable.

In the case $q > 0$ the instability resulting from $p = 0$ corresponds to the analytical instability. However, the high frequency instabilities resulting from $p > 0$ have no analytical counterpart and should be avoided. Accordingly, consider $p = 1$ and bear in mind that the highest value of μ^2 present in the computation is

$$\mu_{-N/2}^2 = \left(\frac{2\pi(-N/2)}{L}\right)^2 = \frac{\pi^2}{h^2}.$$

Hence the condition

$$\tau < \frac{h^2}{\pi} \tag{70}$$

insures that (69b) is not satisfied for any $p > 0$, and therefore that the solution is stable against high frequency perturbation.

Similarly, in the case $q<0$ no analytical instabilities occur and the condition

$$\frac{\tau}{2\theta+\pi}<\frac{h^2}{\pi^2} \tag{71}$$

prevents any numerical instability.

We point out that the conditions (70) and (71) are sufficient, but not necessary. If $|\theta|/\tau$ is small, the range of values of μ^2 for which (69b) is satisfied is small. It could therefore be that no higher frequencies μ_n fall inside this range when (70) or (71) is violated. In this case, of course, the instability will not show up.

6. Numerical experiments. In this section the validity of the stability conditions derived in §§ 4.3 and 5.3 is verified numerically. For this purpose, we consider the x-independent solution

$$u(x,t)=\frac{1}{2}\exp\left(\frac{iqt}{4}\right) \tag{72a}$$

of the NLS, with initial condition

$$u(x,0)=\tfrac{1}{2}. \tag{72b}$$

As was pointed out earlier, both the split-step finite difference and the split-step Fourier methods are, in theory, able to solve the NLS with initial condition (72b) exactly.

The numerical experiments to be reported here consist of solving the NLS after perturbing the initial condition (72b) to

$$u(x,0)=\tfrac{1}{2}(1+\varepsilon(x,0))$$

where the perturbation ε will take any of the following three forms:

(73a) A. $\varepsilon=0$,

(73b) B. $\varepsilon=0.1\cos\dfrac{2\pi x}{L}, \qquad -\dfrac{L}{2}\leqq x\leqq\dfrac{L}{2},$

(73c) C. $\varepsilon=\begin{cases}0.1\left(1-\dfrac{2x}{L}\right), & 0\leqq x\leqq\dfrac{L}{2},\\ 0.1\left(1+\dfrac{2x}{L}\right), & -\dfrac{L}{2}\leqq x\leqq 0.\end{cases}$

In case A it is assumed that a perturbation will be introduced by rounding error. The parameter L in B and C may be varied to regulate the frequency of the perturbation. The difference between B and C lies in the fact that B introduces energy only into the lowest frequency component, whereas C introduces energy into all frequency components present in the computation. The numerical results to be described here will be represented graphically. In each instance the modulus of the numerical solution $|U_j^m|$ will be shown in part (a) of the figure, whereas the discrete Fourier transform $|\hat{U}_n^m|$ will be shown in part (b). The transform will only be shown for positive n, since we have by symmetry of the solution that $|\hat{U}_n^m|=|\hat{U}_{-n}^m|$ for all $n=-N/2,\cdots,N/2-1$. We consider the split-step finite difference and split-step Fourier solutions separately.

6.1. Instability of the split-step finite difference method. In order to verify (38) we use perturbation B and the following choice of parameters: $q=2.0$, $\tau=0.005$, $L=16$

and $N = 50$. Thus all modes n are unstable for which

$$0 < \frac{625}{32} \sin^2 \frac{n\pi}{50} < \frac{1}{2} \tag{74}$$

is satisfied. This implies $|n| = 1, 2$ are unstable. We recall that this instability is a reflection of the analytical instability (12). Figure 1 shows the well-known recurrence associated with the instability. It is clear that the initial condition is approximately reconstructed at $t \approx 18$ after which time the process is repeated periodically. For more comprehensive numerical experiments on this phenomenon the reader is referred to Yuen and Ferguson [7]. We need only point out that the mode $|n| = 1$ becomes unstable first, resulting in a single hump in the solution. Then the second mode $|n| = 2$ starts to dominate, and the instability appears as two humps in the solution.

It should be mentioned that the numerical solution is not able to simulate the periodicity in time indefinitely due to numerical error. Experiments indicate that the finer the grid is, the longer the periodicity can be maintained.

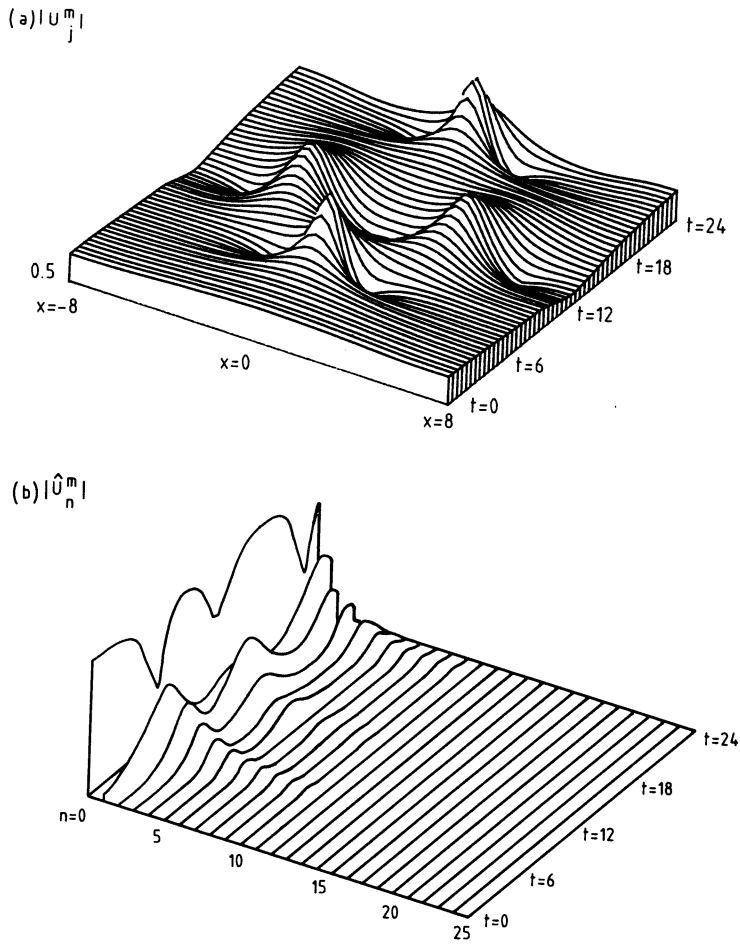

FIG. 1. *Split-step finite difference solution of the NLS with initial condition* $u(x, 0) = 0.5(1 + 0.1 \cos \pi x/8)$.

$q = 2.0 \quad L = 16 \quad \tau = 0.005$

$a = 0.5 \quad N = 50$

It is also of interest to investigate whether rounding error may serve as a perturbation to trigger instability. We therefore use the initial condition (72b) corresponding to the solution (72a). All parameters remain unchanged from the preceding run, with the exception that τ is now taken to be $\tau = 0.02$. The result of this experiment is shown in Fig. 2. For a relatively long time ($0 < t < 30$) no instabilities show up. However, at this stage two humps suddenly appear on the uniform wave train, reminiscent of the two humps in Fig. 1. Apparently it takes some time for the rounding error to introduce energy to the unstable low modes. In this case $|n| = 2$ is triggered first and starts to grow exponentially as predicted by (74). Hence the two humps. After energy has been fed into the unstable low frequencies, the further development proceeds in much the same way as in Fig. 1. The result of this experiment, and in particular the time at which the first instability appears, could be dependent on the procedure by means of which the linear system (22) is solved. In this instance a Gaussian elimination procedure was employed.

Incidentally, we mention that an experiment similar to the present one was conducted by Fornberg and Whitham [28], for a modified version of the Korteweg-de Vries equation.

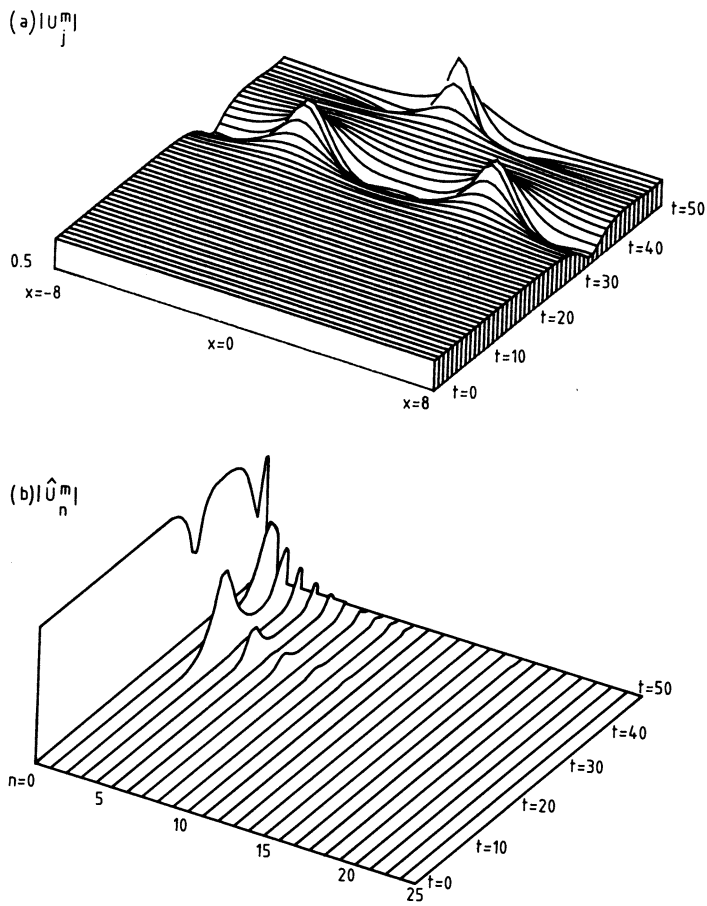

FIG. 2. *Split-step finite difference solution of the* NLS *with initial condition* $u(x, 0) = 0.5$.

$q = 2.0 \quad L = 16 \quad \tau = 0.02$

$a = 0.5 \quad N = 50$

It remains to verify the instability results for the case $q<0$. We recap that in this case instability is expected in those modes for which (39) is satisfied. These instabilities are high frequency instabilities due to numerical error, and may be prevented by the condition (42). In order to investigate the validity of condition (42), we use the initial condition (72b). The following choices for the parameters were made: $q=-4.0$, $L=1$ and $N=20$. Accordingly the condition (42) becomes

$$\tau<\frac{1}{20\sqrt{2}}=0.0354. \tag{75}$$

Two experiments were conducted, with time steps taken to be, respectively, $\tau=0.036$ and $\tau=0.035$. In the former case, which violates (75), a high frequency instability is induced by rounding error and appears at $t\approx 45$. This is shown in Fig. 3. According to (39), the modes $|n|=9$ and $|n|=10$ are unstable. These are precisely the modes which undergo growth in Fig. 3b. Apparently the instability remains restricted to the high modes with no significant leakage to the stable, low modes. Also, the uniform solution is approximately recovered at $t\approx 60$ and $t\approx 150$, resembling the phenomenon of recurrence.

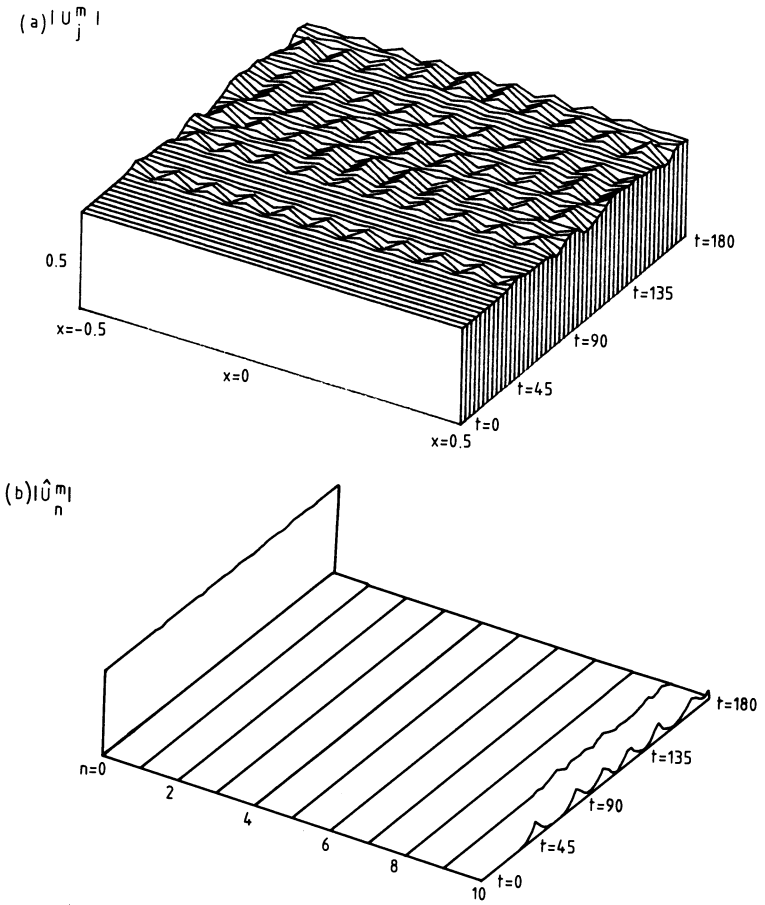

FIG. 3. *Split-step finite difference solution of the* NLS *with initial condition* $u(x,0)=0.5$.

$q=-4.0$ $\quad L=1$ $\quad \tau=0.036$

$a=0.5$ $\quad N=20$

When a time step of $\tau = 0.035$ was used, thereby satisfying (75), no instability in a trial run of 5,000 time steps could be detected. It is therefore concluded that the result (42) is useful, and should be adhered to when solving wave train solutions of the NLS with negative values of q.

6.2. Instability of the split-step Fourier method. The essence of § 5.3 is summarized in the results (70) and (71), which correspond, respectively, to the cases $q > 0$ and $q < 0$. These conditions prevent any unwanted high frequency instabilities in the numerical solution.

To check the validity of (70), we consider an initial condition of the form (72b), with the perturbation given by C, i.e., energy is introduced into all modes. The various parameters were chosen to be: $q = 2.0$, $L = 16$ and $N = 30$. Thus (70) is given by

$$\tau < \frac{64}{225\pi} = 0.0905. \tag{76}$$

We investigated two choices of the time step namely $\tau = 0.090$ and $\tau = 0.091$.

We first consider the time step which satisfies (76), namely $\tau = 0.090$. According to (65) the only unstable modes are the two modes of lowest frequency which is of

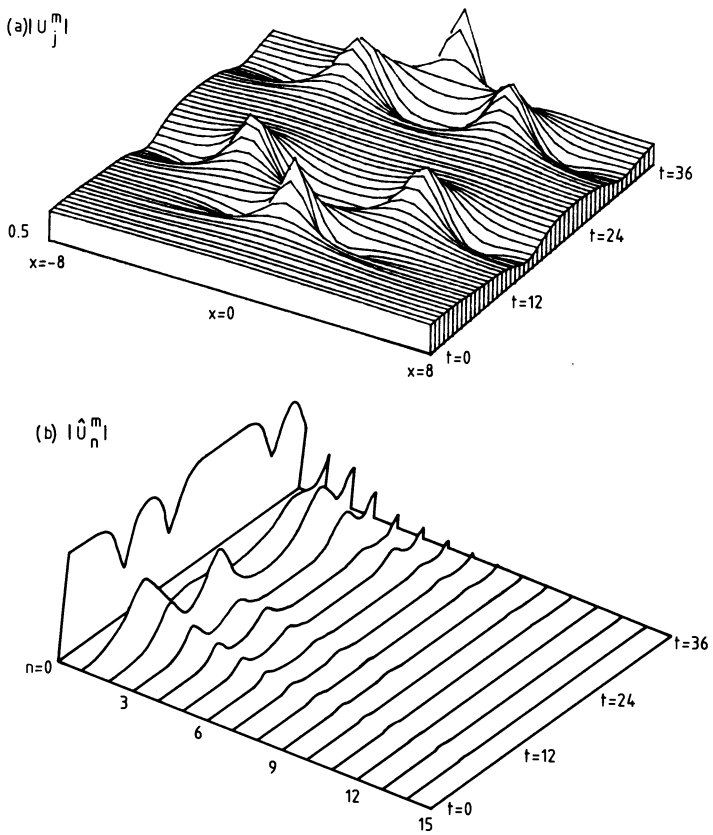

FIG. 4. *Split-step Fourier solution of the* NLS *with initial condition*

$$u(x,0) = \begin{cases} 0.5[1+0.1(1-x/8)], & 0 \leqq x \leqq 8, \\ 0.5[1+0.1(1+x/8)], & -8 \leqq x \leqq 0. \end{cases}$$

$q = 2.0 \quad L = 16 \quad \tau = 0.090$

$a = 0.5 \quad N = 30$

course a reflection of the analytical instability. This is confirmed by Fig. 4. A comparison of Figs. 4 and 1 shows that the behaviour is essentially the same. Most of the energy is transferred between the unstable modes with intermittent returns to the initial condition. However, the similarities remain only for a short time. The long time evolution ($t > 27$) of the two solutions is different, in particular, the order in which the unstable modes dominate. Here some explanation concerning the long time behaviour in Fig. 4 is required. Because of the rather coarse grid ($\tau = 0.09$, $h = 0.53$) it should not be expected that the numerical solution is mimicking the true solution accurately in the later stages. Although the condition (70) is thus clearly capable of preventing the high frequency numerical instability, it does not guarantee high accuracy. It is for this reason that no undue importance should be attached to the differences between Figs. 1 and 4. Subsequently we changed the time step to $\tau = 0.091$. From (65) it follows that in addition to the two analytically unstable modes corresponding to $|n| = 1$ and $|n| = 2$, a high frequency numerical instability corresponding to $|n| = 15$ is also possible. This is confirmed by Fig. 5. After the return to the initial condition, $t \approx 18$, the high frequency component suddenly becomes unstable, resulting in the highly oscillatory appearance of the solution. Again, the growth in the high frequency component seems to be inhibited by the conservation property of the numerical scheme.

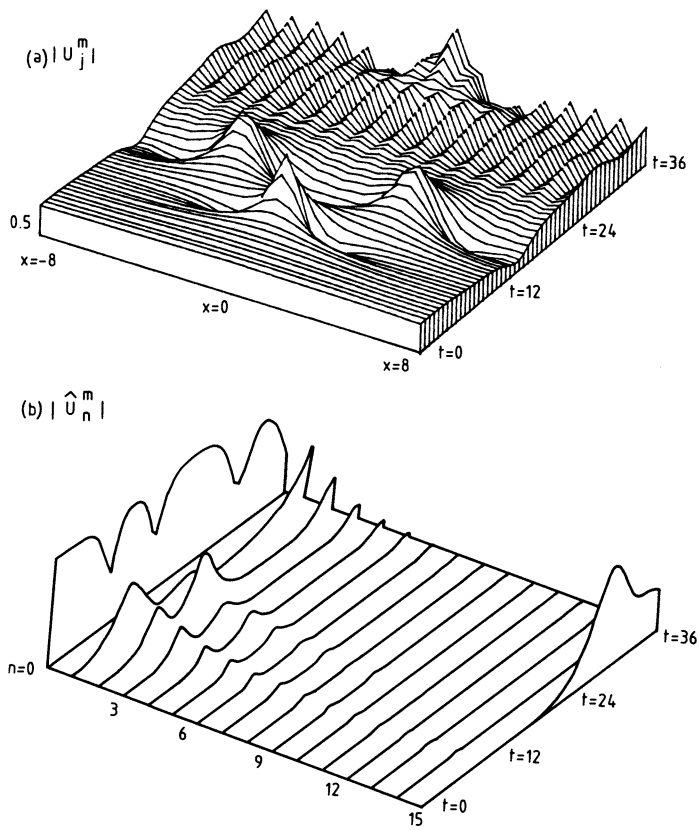

FIG. 5. *Split-step Fourier solution of the* NLS *with initial condition*

$$u(x,0) = \begin{cases} 0.5[1+0.1(1-x/8)], & 0 \leqq x \leqq 8, \\ 0.5[1+0.1(1+x/8)], & -8 \leqq x \leqq 0. \end{cases}$$

$q = 2.0 \quad L = 16 \quad \tau = 0.091$

$a = 0.5 \quad N = 30$

Finally, we turn to the condition (71) which avoids numerical instability in the case $q<0$. This result is verified by the following strategy. We take the initial condition (72b) with perturbation C, and choose $q=-2.0$, $N=20$ and $\tau=0.05$. Next we consider two choices for L—one which satisfies (71), namely $L=8$, and one which does not, namely $L=7.98$. According to the analysis of § 2.3, the theoretical solution ought not to exhibit exponential growth, since $q<0$. In the case $L=8$ this is found to be the case. The perturbation remains neutrally stable. Because of its rather uninteresting appearance the picture is not reproduced here.

On the other hand, in the case $L=7.98$ Fig. 6 shows that the mode of highest frequency ($|n|=10$) does grow as predicted by (65). Note also the return to the initial state at $t\approx 35$, and that the energy growth appears to be restricted to the unstable mode.

In these experiments we have verified two aspects of the analyses of §§ 4.3 and 5.3. Firstly, we have verified that the analytical instability of the NLS is accurately reflected in the numerical solution. In Figs. 1 and 4 our analyses predicted the initial growth, the number of unstable modes and also established that the instability will

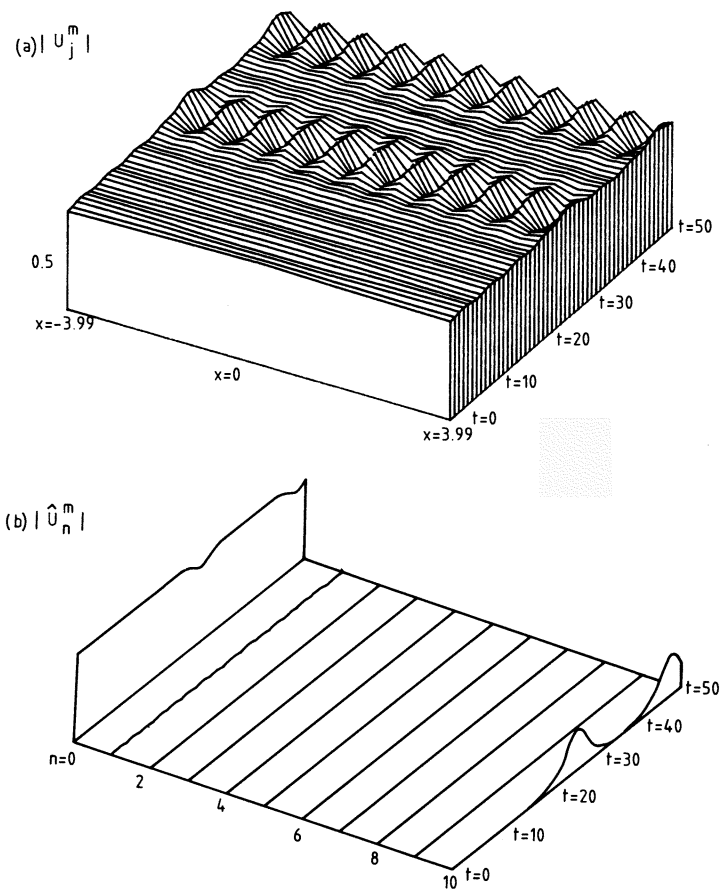

FIG. 6. *Split-step Fourier solution of the* NLS *with initial condition*

$$u(x,0)=\begin{cases}0.5[1+0.1(1-x/3.99)], & 0\leqq x\leqq 3.99,\\ 0.5[1+0.1(1+x/3.99)], & -3.99\leqq x\leqq 0.\end{cases}$$

$q=-2.0 \qquad L=7.98 \qquad \tau=0.05$

$a=0.5 \qquad N=20$

not become unbounded since the schemes are energy conserving. Secondly, we have verified that numerical instability may be encountered, and that the restrictions which may be used to prevent it are accurate.

7. Conclusions. In this paper we investigated two split-step methods for various physical properties represented by the NLS. These properties are all related to the physical phenomenon (the modulation of weakly nonlinear waves in dispersive systems) modelled by the NLS. They are conservation of energy, dispersion and instability.

It was shown that both methods conserve energy exactly in theory. This is especially relevant in the problem of recurrence, where the growth in the low frequencies must be counteracted by conservation to produce the periodic return to the initial state. Even the growth of the high frequency numerical instabilities was shown to be inhibited by conservation to produce recurrent behaviour. It is also known that when a numerical scheme does not conserve energy the solution may become unbounded [17].

Dispersion plays a crucial part in the phenomena modelled by the NLS, see, for example, [3]. The specific type of solution of the NLS (number of solitons, bound states of more than one soliton, etc.) depends on the balance between dispersion and nonlinearity. The accuracy with which the nonlinear dispersion relation is approximated by the numerical method is an indication of its ability to maintain this balance. Dispersion relations were obtained for both numerical methods and these were shown to be exact in the case of the Fourier method, and a good approximation in the case of the finite difference method.

The analytical instability of the NLS which describes the instability of periodic waves on deep water, was shown to be reflected in both numerical schemes. In addition it was shown that the numerical methods contain numerical instabilities which have no analytical counterpart. Criteria to avoid these instabilities were obtained for both methods. The validity of these criteria was demonstrated numerically. We also obtained the result reported earlier by Fornberg and Whitham [28]. Under conditions which do not allow any numerical instabilities according to our analysis, numerical errors accumulated sufficiently to trigger the analytically unstable modes.

We emphasized that in deriving our stepsize restrictions we have linearized around a uniform wave train solution of the NLS. The question arises as to what extent the stepsize restrictions have applicability to more general problems. This forms part of the fundamental question concerning the relevance of linear instability results to the actual nonlinear instability of the NLS. In the analytic case this appears to be an open question. Infeld [32] reviews this problem in detail, and draws the conclusion that no simple answer exists. In the numerical case we should thus warn that it is not clear what relevance the stepsize restrictions have in more general problems. In particular one suspects that the restrictions may have little significance for the computation of solitons. The reason is that if the amplitude of the soliton is small, the solution may be considered as a perturbation of the zero solution. By taking $a = 0$ in our analyses one finds that no instability, neither analytical nor numerical, is predicted (cf. (38), (65)). Hence no restrictions on the step size are placed for solitons of small amplitude. Of course, solitons with moderate to large amplitudes fall outside the scope of linear methods.

Thus we make no claim to the general applicability of the stepsize restrictions we derived, but they are certainly accurate when applied to the class of problems we consider, as the numerical experiments illustrated. The analysis of this report is therefore believed to provide insight into the computation of modulational instability and recurrence phenomena associated with the NLS.

Acknowledgments. We are grateful for the valuable discussions with Professor A. R. Mitchell and to Mr. M. F. Maritz for assistance with the computer graphics. We are also indebted to the referees for constructive remarks.

REFERENCES

[1] T. B. BENJAMIN AND J. E. FEIR, *The disintegration of wave trains on deep water. Part* 1, *Theory*, J. Fluid Mech., 27 (1967), pp. 410–430.

[2] H. HASIMOTO AND H. ONO, *Nonlinear modulation of gravity waves*, J. Phys. Soc. Japan, 33 (1972), pp. 805–811.

[3] R. K. DODD, J. C. EILBECK, J. D. GIBBON AND H. C. MORRIS, *Solitons and Nonlinear Wave Equations*, Academic Press, London, 1982.

[4] G. B. WHITHAM, *Linear and Nonlinear Waves*, John Wiley, New York, 1974.

[5] H. C. YUEN AND B. M. LAKE, *Nonlinear deepwater waves: Theory and experiment*, Phys. Fluids, 18 (1975), pp. 956–960.

[6] B. M. LAKE, H. C. YUEN, H. RUNGALDIER AND W. E. FERGUSON, *Nonlinear deep-water waves; theory and experiment. Part* 2. *Evolution of a continuous wave train*, J. Fluid Mech., 83 (1977), pp. 49–74.

[7] H. C. YUEN AND W. E. FERGUSON, *Relationship between Benjamin-Feir instability and recurrence in the nonlinear Schrödinger equation*, Phys. Fluids, 21 (1978), pp. 1275–1278.

[8] E. FERMI, J. PASTA AND S. ULAM, *Studies of nonlinear problems* I. Reprinted in Nonlinear Wave Motion, A. C. Newell, ed., AMS. Providence, RI, 1974.

[9] H. C. YUEN AND B. M. LAKE, *Instabilities of waves on deep water*, Am. Rev. Fluid Mech., 12 (1980), pp. 303–334.

[10] V. E. ZAKHAROV AND D. B. SHABAT, *Exact theory of two-dimensional self-focusing and one-dimensional self-modulation of waves in nonlinear media*, Soviet Physics JETP, 34 (1972), pp. 62–69.

[11] J. W. MILES, *An envelope soliton problem*, SIAM J. Appl. Math., 41 (1981), pp. 227–230.

[12] B. M. HERBST, A. R. MITCHELL AND J. LL. MORRIS, *Numerical experience with the nonlinear Schrödinger equation*, Report NA/73, University of Dundee, 1983.

[13] F. D. TAPPERT, *Numerical solutions of the Korteweg-de Vries equation and its generalizations by the split-step Fourier method*, Lect. Appl. Math. Am. Math. Soc., 15 (1974), pp. 215–216. See also R. H. HARDIN, F. D. TAPPERT, *Applications of the split-step Fourier method to the numerical solution of nonlinear and variable coefficient wave equations*, SIAM Rev., Chronicle 15 (1973), p. 423.

[14] J. M. SANZ-SERNA, *An explicit finite difference scheme with exact conservation properties*, J. Comp. Phys., 52 (1982), pp. 273–289.

[15] J. M. SANZ-SERNA AND V. S. MANORANJAN, *A method for the integration in time of certain partial differential equations*, J. Comp. Phys., 52 (1983), pp. 273–289.

[16] M. DELFOUR, M. FORTIN AND G. PAYRE, *Finite difference solutions of a nonlinear Schrödinger equation*, J. Comp. Phys., 44 (1981), pp. 277–288.

[17] D. F. GRIFFITHS, A. R. MITCHELL AND J. LL. MORRIS, *A numerical study of the nonlinear Schrödinger equation*, Comp. Methods in Appl. Mech. and Eng., 45 (1984), pp. 177–215.

[18] B. M. HERBST, A. R. MITCHELL AND J. A. C. WEIDEMAN, *On the stability of the nonlinear Schrödinger equation*, J. Comp. Phys, to appear.

[19] J. M. SANZ-SERNA, *Methods for the numerical solution of the nonlinear Schrödinger equation*, Math. Comp., 43 (1984), pp. 21–27.

[20] A. R. MITCHELL AND J. LL. MORRIS, *A self adaptive difference scheme for the nonlinear Schrödinger equation*, Arab Gulf Journal of Scientific Research, 1 (1983), pp. 461–472.

[21] T. R. TAHA AND M. J. ABLOWITZ, *Analytical and numerical aspects of certain nonlinear evolution equations.* II. *Numerical, nonlinear Schrödinger equation.* J. Comp. Phys., 55 (1984), pp. 203–230.

[22] G. STRANG, *On the construction and comparison of difference schemes*, this Journal, 5 (1968), pp. 506–517.

[23] A. R. GOURLAY, *Splitting methods for time dependent partial differential equations*, in The State of the Art in Numerical Analysis, D. Jacobs, ed Academic Press, New York, 1977.

[24] R. J. LEVEQUE AND J. OLIGER, *Numerical methods based on additive splitting for hyperbolic partial differential equations*, Math. Comp., 40 (1983), pp. 369–497.

[25] R. VICHNEVETSKY AND J. B. BOWLES, *Fourier Analysis of Numerical Approximations of Hyperbolic Equations*, SIAM Studies 5, Society for Industrial and Applied Mathematics, Philadelphia, 1982.

[26] D. GOTTLIEB AND A. ORZAG, *Numerical Analysis of Spectral Methods: Theory and Applications*, CBMS Regional Conference Series in Applied Mathematics 26, Society for Industrial and Applied Mathematics, Philadelphia, 1977.

[27] B. FORNBERG, *On a Fourier method for the integration of hyperbolic equations*, this Journal, 12 (1975), pp. 509–528.
[28] B. FORNBERG AND G. B. WHITHAM, *A numerical and theoretical study of certain nonlinear wave phenomena*, Phil. Trans. Roy. Soc. Lond. 289 (1978), pp. 373–404.
[29] J. M. SANZ-SERNA AND J. G. VERWER, *Conservative and nonconservative schemes for the solution of the nonlinear Schrödinger equation*, IMA J. Num. Anal., to appear.
[30] S. D. CONTE AND C. DE BOOR, *Elementary Numerical Analysis. An Algorithmic Approach*, third ed., McGraw-Hill, New York, 1980.
[31] E. O. BRIGHAM, *The Fast Fourier Transform*, Prentice-Hall, Englewood Cliffs, NJ, 1974.
[32] E. INFELD, *Nonlinear waves: from hydrodynamics to plasma theory*, in Advances in Nonlinear Waves, Vol. I, L. Debnath, ed., Pitman, Boston, 1984.